

## Fabrication and Characterization of Nano-SiC/ Thermoplastic Polyurethane Hybrid Heating Membranes Based on Fine Silver Filaments

Liu Hao,<sup>1,2</sup> Wang Xin,<sup>1</sup> Li Jin,<sup>1,2</sup> Kang Weimin,<sup>1,2</sup> Cheng Bowen,<sup>1,2</sup> Hao Lei,<sup>1</sup> Xu Yan<sup>1</sup>

<sup>1</sup>Department of Textile Engineering, School of Textiles, Tianjin Polytechnic University, Tianjin 300387, China

<sup>2</sup>Department of Textile Engineering, Key Laboratory of Advanced Textile Composite Materials, Ministry of Education, Tianjin Polytechnic University, Tianjin 300387, China

Correspondence to: L. Hao (E-mail: liuhao@tjpu.edu.cn) and L. Jin (E-mail: lijn@tjpu.edu.cn)

**ABSTRACT:** A novel method for fabricating flexible and waterproof heating membranes was presented in this study, nano-SiC/thermoplastic polyurethane (TPU) hybrid membranes has been successfully prepared by pouring modified nano-SiC/TPU solution into a mold with 0.05 mm silver filaments. Nano-SiC particles were modified using silane coupling agent, subsequently, were dispersed evenly in the solvent, average diameter of nano-SiC particles could reach 180.4 nm. Fourier Transform Infrared spectra showed organo-functional groups were grafted on surface of nano-SiC by covalent bond. TPU membrane with 10 wt % nano-SiC had the highest decomposition temperature, and maximum stress. Thermal conductivity and the surface equilibrium temperature under the same loaded voltage of membranes ascended with increasing of nano-SiC content. Flexible, waterproof nano-SiC/TPU heating membranes have wide application prospect in active warming garments and other fields required flexible heating elements. © 2014 Wiley Periodicals, Inc. *J. Appl. Polym. Sci.* 2015, 132, 41498.

**KEYWORDS:** grafting; manufacturing; membranes; polyurethanes; thermal properties

Received 25 March 2014; accepted 4 September 2014

DOI: 10.1002/app.41498

### INTRODUCTION

Smart textiles and clothing which can monitor change of environment parameters, such as temperature and pressure, etc, and make appropriate response to protect human body will have wide application prospect in future. Metals and conducting polymer filament or yarn have already been used in many smart textiles and garments, for example, heating garments, antistatic textiles, electromagnetic interference shielding, transport of electrical signals, sensors, etc.<sup>1–3</sup> With the progress of material science and electrical technology, active warming garments will become more lightweight and intelligent. In the last decades, many researchers have paid increasing attention in heating fabrics and heating garments. Hewitt<sup>4</sup> fabricated a flexible electric heating pad by using resistance wire and a flexible fabric support as early as 1929, Andre<sup>5</sup> developed a heating fabric by arranging nonconductive threads as warp, and nonconductive threads strip and conductive threads strip as weft alternately. More and more heating fabrics and heating garments were springing up, especially in recent years. Stainless steel yarns with comb structure were arranged in cotton yarn fabric during the weaving process to acquire heating element.<sup>6</sup> Hao et al.<sup>7</sup>

integrated superfine silver filament in woven fabric and fabricated a resistance adjustable flexible heating fabric, experimental results showed strong positive linear correlations are between rated power and utmost ascending temperature of flexible heating fabric and between power consumption and presetting equilibrium temperatures of flexible heating fabric. Hamdani et al.<sup>8</sup> conducted on a study of the thermo-mechanical properties of knitted structures, the methods of manufacture, effect of contact pressure at the structural binding points, on the degree of heating, and utilized infrared images to study the heat distribution over the surface of the knitted fabrics.

The conductive filaments or yarns in above described heating fabrics are exposed directly in air, short-circuit may result in destruction of heating fabrics or controlling circuits when heating fabrics is in high humidity environment, moreover, the conductive filaments or yarns are easily corroded by sweat. Therefore, fabrication of flexible, waterproof heating elements has very important significance to widen application of heating fabrics and smart heating garments. Polymer coating on heating fabrics and conductive filaments integrated into polymer membranes are two effective approaches for fabricating waterproof

**Table I.** Average Diameters of Nano-SiC

| Index | Before settlement |           |           | After 12 hours settlement |           |           |
|-------|-------------------|-----------|-----------|---------------------------|-----------|-----------|
|       | SiC               | SiC-KH570 | SiC-KH550 | SiC                       | SiC-KH570 | SiC-KH550 |
| 1     | 1392.6            | 171.5     | 227.7     | 3591.1                    | 343.5     | 447.7     |
| 2     | 1097.6            | 189.2     | 236.5     | 2188.2                    | 343       | 449.3     |
| Mean  | 1245.1            | 180.4     | 232.1     | 2890                      | 343.3     | 448.5     |

heating elements. However, low thermal conductivity of polymers is not good for heat transfer in polymer heating membranes and leads easily to local high temperature, hence, improvement of thermal conductivity of polymer shall be in favor of popularization and application of polymer heating membranes in active warming garments or other fields. Many researchers have focused on enhancing thermal conductivity of polymer by adding nano-particles. Carbon, metallic particles, and ceramic particles can be all filled in polymer to enhance their thermal conductivities. Bian et al.<sup>9</sup> has successfully produced a strong interfacial interaction between the microwave-exfoliated graphite oxide (MEGO) and the thermoplastic polyurethane (TPU) matrix via melt blending followed by injection molding. MEGO layers were homogeneously dispersed throughout the TPU matrix. The results showed that the glass transition temperatures (TG) of the nano-composites increased with increasing MEGO content, and the thermal stabilities, electrical conductivities and mechanical properties of nano-composites were remarkably improved in comparison with pure TPU matrix. Ganguli et al.<sup>10</sup> fabricated chemically functionalized exfoliated graphite-filled epoxy composites with load levels from 2% to 20% by weight, thermal conductivity of composite, increased by 28-fold over the pure epoxy resin at the 20% by-weight load level, increasing from 0.2 to 5.8 W/m K. Veca et al.<sup>11</sup> incorporated commercially available carbon graphite nanosheets with polymers to produce flexible nanocomposites that exhibit record-setting anisotropic thermal conductivities. Han et al.<sup>12</sup> reviewed systematically the thermal conductivity of carbon nanotubes and their polymer nanocomposites. Metallic particles, such as aluminum, silver, copper, and nickel powders, are commonly used for improving thermal conductivity of polymers. Kumlutas et al.<sup>13</sup> investigated numerically the effective thermal conductivity of aluminum filled high-density polyethylene composites as a function of filler concentration. Boudenne et al.<sup>14</sup> investigated the thermal conductivity, diffusivity, effusivity, and specific heat of polypropylene matrix was filled with two different size copper particles. Polymer composites with metallic particles filler or carbon graphite shall be improved in electric conductivity and thermal conductivity, and density of polymer increases also with increasing of metal fillers, hence, application of these filler should be restricted when lightweight of polymer is required. In order to acquire polymer materials with well thermal conductivity and electric insulativity, ceramic nano-particles reinforced polymer materials have been also used extensively as electronic materials. Cao et al.<sup>15</sup> reported a simple method for coating silicon carbide (SiC) nano-particles with polystyrene (PS) to improve the interfacial adhesion between

polymer matrix and SiC nano-particles, the thermal conductivities of the untreated SiC/PS and p-SiC/PS nanoparticles composites increased by about 192% and about 353%, respectively. Saha et al.<sup>16</sup> reported preparation of polyurethane and polyurethane/clay nanocomposites based on polyethylene glycol, isophorone diisocyanate (IPDI), an aliphatic diisocyanate and 1,4- Butanediol as chain extender by solution polymerization. Decomposition temperature (DT) of the PU/clay nanocomposite is much higher than the pristine TPU, the crystallinity in TPU nanocomposite with the incorporation of 3 wt % nano-clay increases, then diminishes with further loading. McCullough et al.<sup>17</sup> added spherical nanometer- and sheet micrometer-sized silver particles to TPU, in the content of 15 wt %, the thermal connection of final composites increased a factor of four to maximum 0.987 W/mK and a factor of 2 to 0.718 W/mK, respectively. Zhou et al.<sup>18</sup> obtained the thermal conduction mechanism of nano-sized SiC/diglycidyl ether of bisphenol-A glycidol ether epoxy resin/2-ethyl-4-methylimidazole composites. Choi et al.<sup>19</sup> acquired a flexible thermal conductive composites multiwalled carbon nanotubes functionalized with amino groups (MWCNT-NH<sub>2</sub>), A thermal conductivity of 3.81 W/mK was achieved at an MWCNT-NH<sub>2</sub> loading of 3 wt % and micro-AlN loading of 70 wt % while their flexibility was maintained. All of the composites fabricated by the optimized process endured about 200,000 bending cycles without rupturing or losing their thermal conductivity. Some ceramic materials such as aluminum nitride (AlN), boron nitride (BN), and silicon carbide (SiC) were paid more attention as thermal conductive fillers because of their high thermal conductivity and electrical resistivity.<sup>20</sup> Certain factors, such as filler packing density,<sup>21</sup> particle size, and size distribution approach,<sup>22</sup> surface treatment approaches,<sup>23</sup> and nano-particles mixing methods,<sup>24</sup> etc., which affected the thermal conductivities of composites with ceramic filler were reported.

Smart heating garments which can keep warmth for outdoor workers in extremely cold environments, soldiers, elderly and rheumatic diseases will have wide application prospect in the future. However, conductive filaments in heating textiles are normally exposed in air that causes easily short circuit or other dangers because of sweat. In this work, SiC nano-particles will be filled into the TPU to improve the thermal conductivity of SiC/TPU hybrid membrane, and a waterproof and flexible hybrid heating membrane will be obtained by enclosing the silver filaments into optimal proportion of SiC/TPU hybrid membrane which can improve the stability and robustness of heating garments.

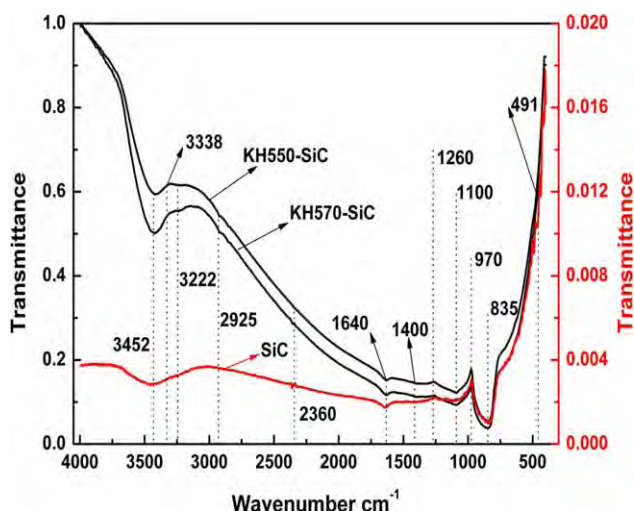


**Figure 1.** FTIR spectra of modified and unmodified nano-SiC particles. [Color figure can be viewed in the online issue, which is available at [wileyonlinelibrary.com](http://wileyonlinelibrary.com).]

## EXPERIMENTAL

### Materials

TPU was purchased from ShenZhen Resin, ShenZhen, China. Molecular architecture of TPU is composed of alternately hard segments and soft segments. Soft segments were obtained by polyreaction of methylene diphenyl diisocyanate (MDI), toluene diisocyanate (TDI), and macromolecular polyol, and hard segments were obtained by adding chain extender. We selected 60 A TPU with well elasticity. The nano-SiC particles (from Aipurui Nano-Material, Nanjing, China) have average diameter of 100 nm. Silane coupling agents [ $\gamma$ -aminopropyl-triethoxy sil-

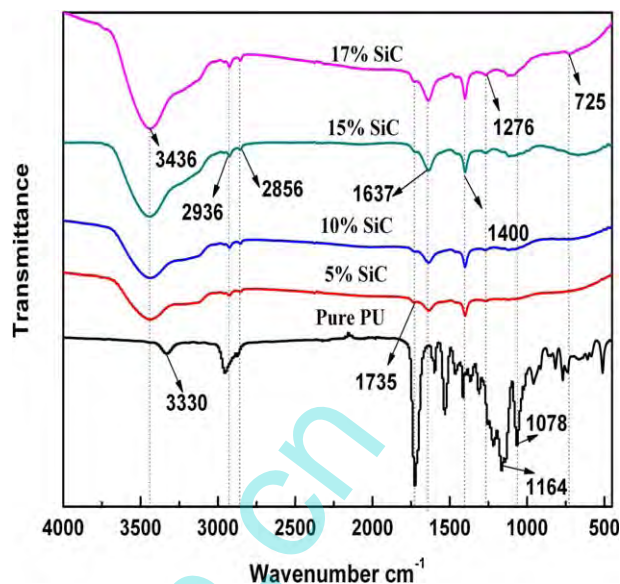


**Figure 3.** FTIR spectra of TPU membranes with different content nano-SiC fillers. [Color figure can be viewed in the online issue, which is available at [wileyonlinelibrary.com](http://wileyonlinelibrary.com).]

ane (KH550) and  $\gamma$ -propyl methyl acryloyl oxygen radicals silane (KH570)] were purchased from Beijing Chemical Reagent, China, other all chemically pure solvents were acquired from Tianjin KeMiOu Chemical Agent, China.

### Surface Modification of Nano-SiC Particles

Nano-SiC particles agglomerated easily into solvent because of existence of van der Waals force, coulomb force, and chemical bonding force between particles, hence, surface chemical modification is necessary for nano-SiC particles. First, Nano-SiC particles were dried in vacuum oven at 120°C for 12 hours, dispersed in anhydrous ethanol/water (1 : 1 mass ratio) mixture solution which was loaded in a round bottom flask with three necks by high power ultrasonic cleaner for 30 min, 3 wt % saline couple agent KH550 or KH570 were poured into the flask, subsequently, the mixture solution in flask was stirred on magnetic stirrer in constant temperature water bath at 70°C for 5 hours. Finally, the surface modified nano-SiC particles were rinsed repeatedly using absolute ethanol on high speed tabletop centrifuge, and dried in vacuum at 50°C for 12 hours, then ground in mortar and stored in desiccator.

### Fabrication of SiC/TPU Hybrid Membranes and Heating Membranes

The nano-SiC/TPU hybrid membrane is fabricated by solution blending method. Sixty grams TPU particles and 240 mL Dimethyl Formamide (DMF) were put in 500 mL breaker and were stirred by mechanical raking until TPU particles were dissolved completely in DMF solution. Surface modified nano-SiC particles by KH550 (10 wt %) were dispersed in DMF by ultrasonic dispersion method.

Nano-SiC/DMF solution was poured into TPU/DMF solution, then was diluted to 5, 10, 15, and 17 wt % nano-SiC by adding DMF solvent, mixture solution was removed air bubbles

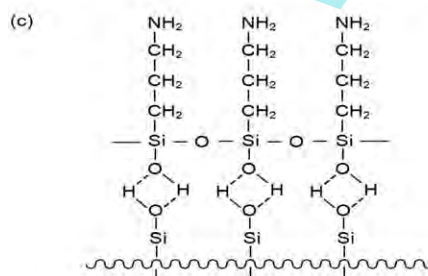
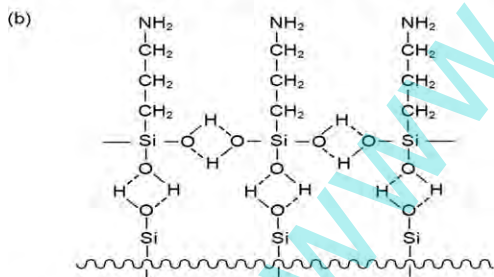
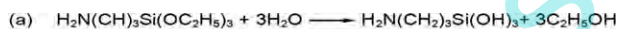


**Figure 2.** Schematic diagram of (a) hydrolysis of KH550, (b) hydrogen bonding of SiC particle and KH550, and (c) dehydrogenation oligomerization of KH550 and SiC particles.

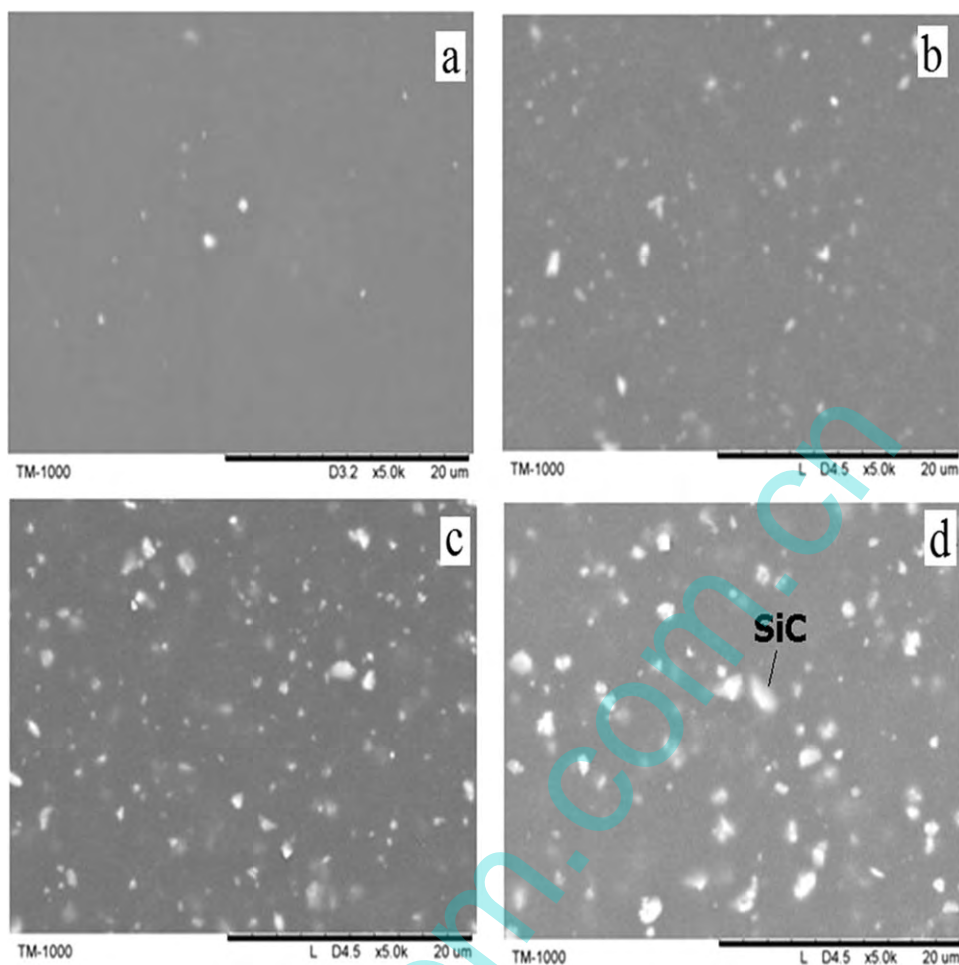


**Figure 4.** SEM images of TPU membranes with (a) 0 wt %, (b) 5 wt %, (c) 10 wt %, (d) 15 wt % nano-SiC.

in vacuum oven for 1 hour, then was poured on dry, clear, and smooth glass mould with or without fine silver filaments, were scraped from right to left evenly along one direction using glass rod, distance between two fine silver filaments is about 8 mm. The glass moulds were put horizontally into 40°C air oven for 3 hours. Silver filaments were integrated in nano-SiC/TPU hybrid membrane as heating resistance wires.

#### Fourier Transform Infrared, Morphology, Thermal Gravimetric, and Mechanical Properties Analysis

Delsa Nano particle size analyzer (BERKMAN Countler, American) was used to measure the diameter of nano-SiC particles in solution. Fourier Transform Infrared (FTIR) spectra of nano-SiC particles and nano-SiC/TPU hybrid membranes were acquired by BRUKER TENSOR 27 (from Bruker corporation, Germany), the scanning frequency range was 4000–400  $\text{cm}^{-1}$ . The surface appearances of SiC/TPU hybrid membranes were measured by atomic force acoustic microscope CSPM5500 (BenYuan nano instrument, China). Thermal gravimetric analysis (TGA) of SiC/TPU hybrid membranes were performed by simultaneous thermal analyzer STA409PC (NETZSCH, Germany) in nitrogen environment from room temperature to 700°C at a rate of 10°C/min. Five pieces of specimens with

50 × 10 mm dimension were acquired from each kinds of SiC/TPU hybrid membrane, and their mechanical properties were measured by using universal strength tester (Instron 3369, USA).

#### Thermal Performance Test of SiC/TPU Hybrid Membranes

The heat conduction of nano-SiC/TPU hybrid membranes was measured by LFA 1000 (Linseis, Germany). Infrared video camera of TP8 (WuHan GaoDe, China) was utilized for acquiring the surface temperature field of heating membranes. Three Volts voltages were loaded on single fine silver filament of four kinds of heating members with 0, 5, 10, and 15 wt % nano-SiC, respectively, subsequently voltages from 1 to 5 V with 1 V interval were loaded on heating membrane with 10 wt % nano-SiC in turn, switch of power source was opened after surface temperature reached equilibrium temperature. In order to decrease amount of infrared images and not to affect the measurement accuracy, the collecting frequency was set at 10 Hz in beginning of heating, at 0.5 Hz in stable stage, at 2 Hz in thermal radiating stage. All contact points were fixed silver filament with aluminum sheets to facilitate testing and were cleaned by alcohol to reduce the measurement error, finally, all nano-SiC/TPU hybrid membranes were fasten on an appropriate size board.

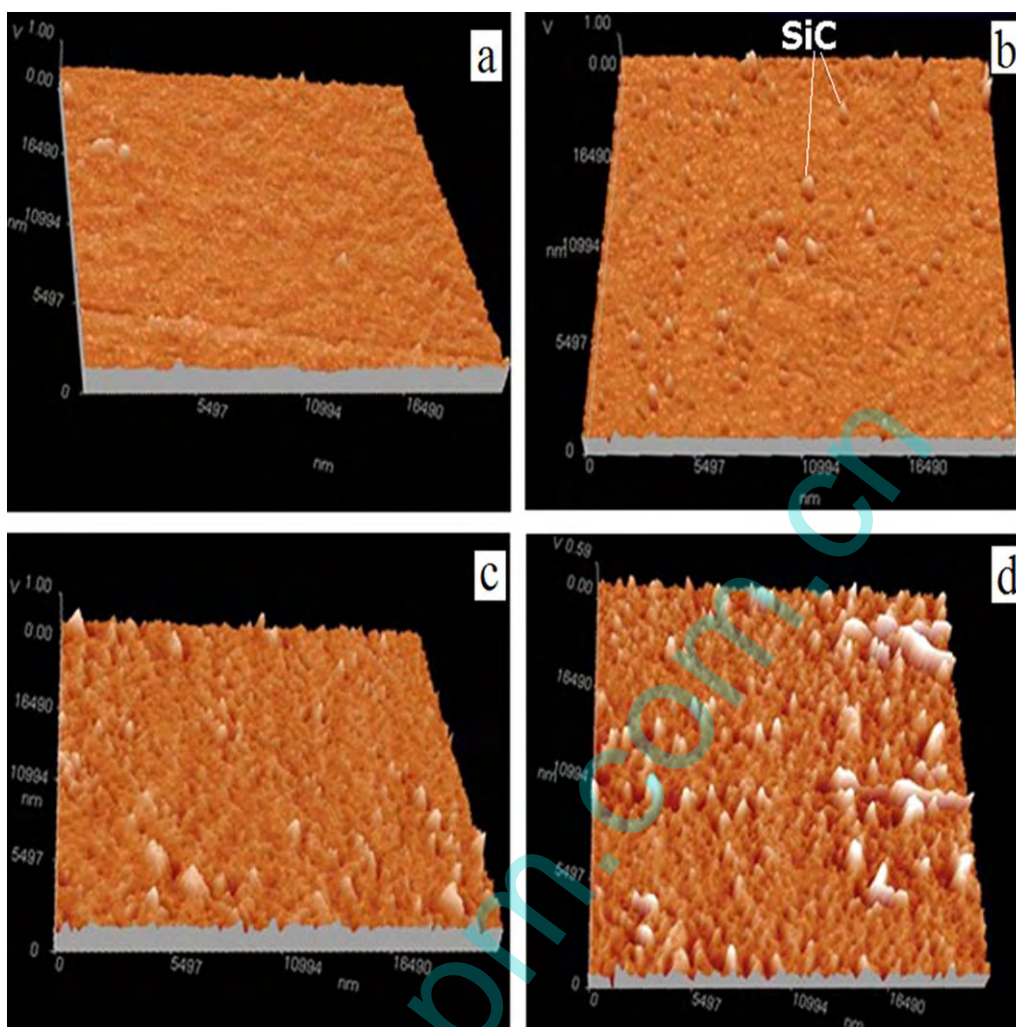


**Figure 5.** AFM images of TPU membranes with (a) 0 wt %, (b) 5 wt %, (c) 10 wt %, (d) 15 wt % nano-SiC. [Color figure can be viewed in the online issue, which is available at [wileyonlinelibrary.com](http://wileyonlinelibrary.com).]

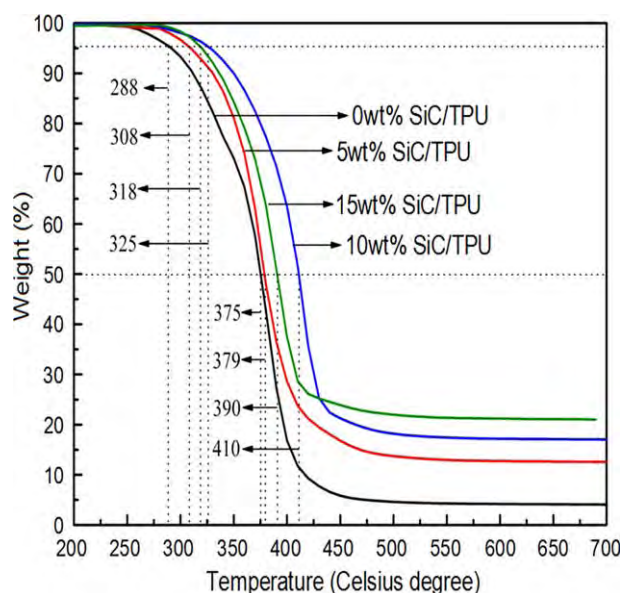
## RESULTS AND DISCUSSION

Table I shows the diameters of nano-SiC and modified nano-SiC using KH570 and KH550 that were dispersed into DMF solvent, the diameters of modified nano-SiC using KH570 reaches 171.5 nm and is approximate 12.3% of that of unmodified nano-SiC. The diameters of nano-SiC after 12 hours sediment are 200–258% of nano-SiC before solution sediment. Obviously, nano-SiC particles modified by KH570 and KH550 have smaller diameter that of unmodified nano-SiC either before solution sediment or after solution sediment, the reasons are that some silanol organo-functional groups were grafted on surface of nano-SiC which makes tensiometric property of nano-SiC depress, so nano-SiC can be dispersed easily into solvent, however, Brownian motion, gravity of nano-SiC and van der Waals force between nano-SiC will lead to agglomeration and sediment, the diameter of SiC particles in solution will increase with sediment time.

Figure 1 shows FTIR spectra of modified nano-SiC particles using KH550 and KH570 and unmodified nano-SiC particles. The intensities of absorption peak at  $3222\text{ cm}^{-1}$  of modified

nano-SiC particles are stronger than that of unmodified nano-SiC particles because of  $-\text{NH}_2$  existence. The bending and stretching vibration absorption band of  $-\text{Si}-\text{O}$  at  $491$  and  $1100\text{ cm}^{-1}$  of modified nano-SiC increased also correspondingly on the FTIR, some absorption peaks such as  $3338$ ,  $1400$ ,  $2360$ , and  $3452\text{ cm}^{-1}$  appear also on the FTIR of modified nano-SiC, which indicates hydrolysate silanol of the silane coupling agent has been grafted successfully on surface of nano-SiC.

A native oxide layer of  $\text{SiO}_2$  is on outer layer of SiC particles, and the percentage of  $\text{SiO}_2$  and  $\text{O}^{2-}$  ions will increase by oxidation. The  $\text{O}^{2-}$  ions exist as nonbridging oxygen: one bond connects with  $\text{Si}^{4+}$  and another bond forms a  $-\text{OH}$  group when reacting with  $\text{H}_2\text{O}$ .<sup>18</sup> The mechanism of silane treatment using KH550 can be described by a grafting model as shown in Figure 2. Hydrolysis of the alkoxide groups of KH550 produces silanol ( $\text{SiOH}$ ) groups [shown in Figure 2(a)], and hydrolyzed molecules form siloxane bonds by condensation reactions. These hydrolyzed molecules were bonded on SiC particles surface by hydrogen bonding, thus one end of KH550 forms hydrogen bonds with the SiC particles [shown in Figure 2(b)]. After the



**Figure 6.** TG spectra of SiC/TPU hybrid membranes. [Color figure can be viewed in the online issue, which is available at [wileyonlinelibrary.com](http://wileyonlinelibrary.com).]

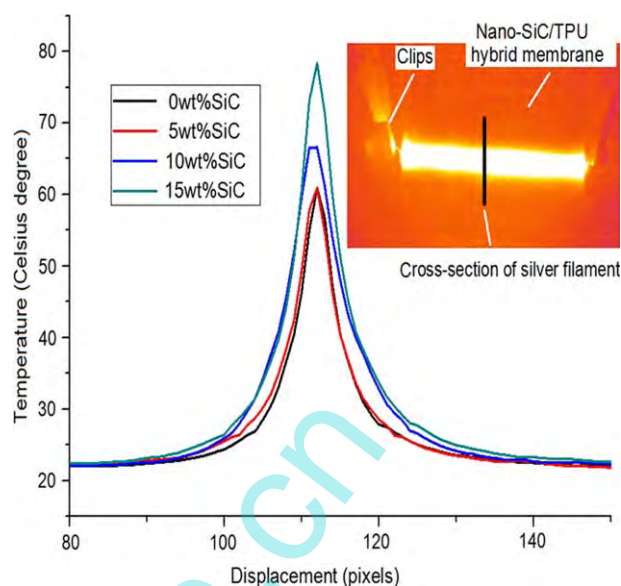
hydrogen bonds between KH550 and SiC particles are heat-induced dehydrated, several layers of coupling agent molecular were grafted on the surface of SiC particles by O-Si covalent bond [shown in Figure 2(c)].

Figure 3 shows that the FTIR spectrum of the membranes with modified nano-SiC fillers is smoother than that of pure TPU membrane between frequency  $1735$  and  $500\text{ cm}^{-1}$ , which can be explained for that the molecular structure changes greatly and keeps balance between soft and hard segments in polymer substrate after incorporating nano-SiC particles. The peak at  $1400$  and  $1637\text{ cm}^{-1}$  are the characteristic absorption peaks of Si-O stretching vibrations and flexural vibrations, respectively. The stretching vibration band  $3436\text{ cm}^{-1}$  of the hydroxyl group because of the noncondensed SiOH and/unreacted -OH groups, and the flexural vibration band  $1637\text{ cm}^{-1}$ , illustrating that the hydroxyl group and the hydrogen bond absorbed on the nano-SiC particles surface were increased with the proportion increasing of the nano-SiC particles. However, absorption peak at  $2936\text{ cm}^{-1}$  of the -CH<sub>2</sub> groups decreases with increasing of nano-SiC particles. Above characters showed organo-functional groups were grafted on surface of nano-SiC particles, and nano-SiC particles have connected with the macromolecules in TPU membrane by chemical covalent bond.

Figure 4 shows that amount and diameter of SiC particles increase with increasing of SiC content. Diameters of SiC particles on surface of TPU membrane with 10 wt % SiC are mostly in the range between 300 and 500 nm, but diameters of

**Table II.** Thermal Conductivities of TPU Membranes with Different Mass Ratio Nano-SiC

| Mass ratio of nano-SiC (wt %) | 0    | 5    | 10   | 15   |
|-------------------------------|------|------|------|------|
| Thermal conductivity(W/mK)    | 0.29 | 0.45 | 0.87 | 0.98 |



**Figure 7.** Cross-section temperature curve of silver filament in nano-SiC/TPU hybrid membrane. [Color figure can be viewed in the online issue, which is available at [wileyonlinelibrary.com](http://wileyonlinelibrary.com).]

a lot of SiC particles is approximate  $2\text{ }\mu\text{m}$  when the content of SiC in TPU membrane is at 15 wt %. Obviously, agglomeration phenomenon is the reason of diameters increasing of SiC particles in TPU membrane. Meanwhile, one can observe the similar result from the AFM images as shown in Figure 5, TPU membrane without SiC [Figure 5(a)] is smoother than other TPU membranes with different proportion SiC particles, amount and dimension of synapses on TPU membranes also increase with increasing of SiC content.

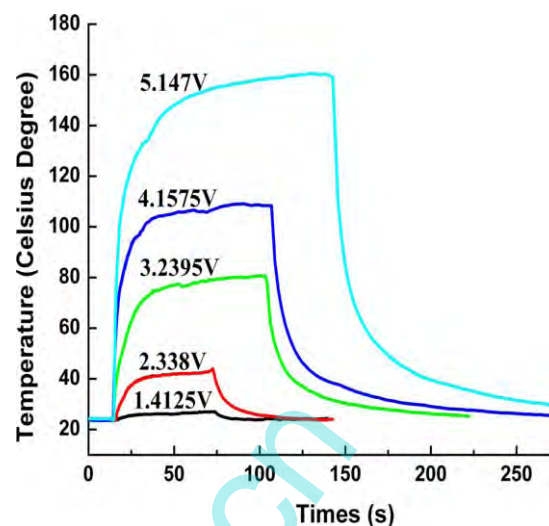
Figure 6 shows the thermal decomposition curve of four kinds of TPU membranes. When the mass loss of hybrid membranes is 5%, the their decomposition temperatures (DTs) are, respectively,  $288^\circ\text{C}$ ,  $308^\circ\text{C}$ ,  $325^\circ\text{C}$ , and  $318^\circ\text{C}$ . When the mass loss of hybrid membranes is 50%, the DTs are, respectively,  $375^\circ\text{C}$ ,  $379^\circ\text{C}$ ,  $410^\circ\text{C}$ , and  $390^\circ\text{C}$ , obviously, measured results showed the thermal stability of TPU hybrid membrane with 10 wt % SiC is the best. The reason is that TPU is a macromolecule material with soft and hard cross-linking segments, modified nano-SiC particles were embedded into molecule structure and three-dimensional network structure was formed as particle-soft segment-particle-hard segment, hence, thermal stability of hybrid membranes were improved with increasing of weight ratio of nano-SiC, however, the DT of TPU hybrid with 15 wt % nano-SiC is less than that with 10 wt % nano-SiC. The reason is probable that the agglomeration of nano-SiC particles becomes more severe when weight ratio of nano-SiC exceeds certain value, three-dimensional network structure between SiC particles and polymer segments can't be constructed well.

Table II shows the thermal conductivity of several nano-SiC/TPU hybrid membranes increases with increasing of nano-SiC, Figure 7 shows temperature lines that is vertical with silver filaments on TPU hybrid membranes with different mass ratio of nano-SiC, one can observe the maximum temperature on silver

**Table III.** Maximum Stress, Elongation at Break, and Initial Modulus of TPU Membranes with Different Proportion of SiC Particles

| Content of SiC (wt %)   | 0                   | 3            | 5            | 7             | 10                 | 13           | 15           | 17           |
|-------------------------|---------------------|--------------|--------------|---------------|--------------------|--------------|--------------|--------------|
| Maximum stress (Mpa)    | 15.4 ± 1.35         | 16.1 ± 2.84  | 16.2 ± 2.91  | 19.3 ± 3.02   | <b>24.4 ± 3.75</b> | 16.3 ± 2.64  | 15.0 ± 5.26  | 14.6 ± 5.22  |
| Elongation at break (%) | <b>956.4 ± 44.6</b> | 818.9 ± 38.7 | 809.3 ± 43.4 | 924.4 ± 109.9 | 905.7 ± 102.1      | 829.6 ± 84.9 | 796.2 ± 99.9 | 745.8 ± 46.8 |
| Initial modulus (Mpa)   | 19.8                | <b>35.0</b>  | 31.0         | 22.3          | 34.2               | 20.6         | 25.9         | 20.0         |

The bold characters denote maximum value in maximum stress, elongation at break, initial modulus of SiC/TPU hybrid membranes with different proportion SiC content.



**Figure 8.** Surface maximum temperatures vs. time of TPU membrane with 10 wt % nano-SiC. [Color figure can be viewed in the online issue, which is available at wileyonlinelibrary.com.]

filament increase with increasing of nano-SiC which is consistent with thermal conductivities on Table II.

Table III shows that the stress of nano-SiC/TPU hybrid membranes reaches the maximum value of 24.4 MPa when nano-SiC content is at 10 wt %, deviations of maximum stress increase with increasing of nano-SiC content, the reason is possible that small size nano-SiC particles can rehabilitate for certain structure defects between polymer segments, thus even distribution of nano-SiC is favor of enhancing the stress and decreasing stress concentration of nano-SiC/TPU hybrid membranes. With further increasing of SiC content, dimension of SiC will increase because of agglomeration effect. Big size SiC particles not only induce stress concentration but also destroy the continuity of

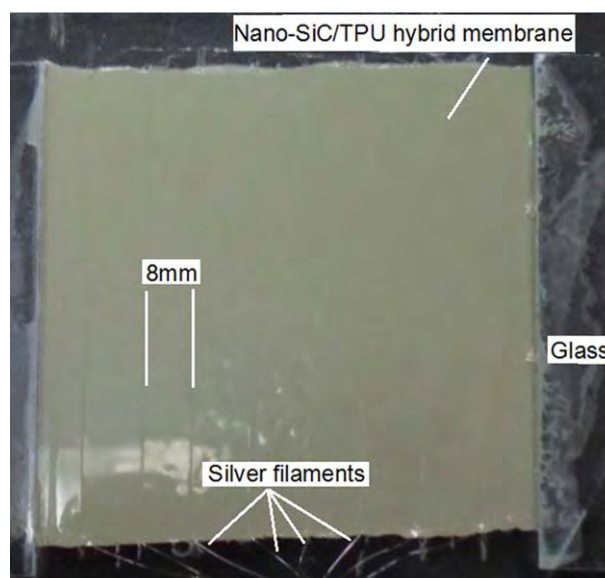


**Figure 9.** Overall view of nano-SiC/TPU membrane with silver filaments. [Color figure can be viewed in the online issue, which is available at wileyonlinelibrary.com.]

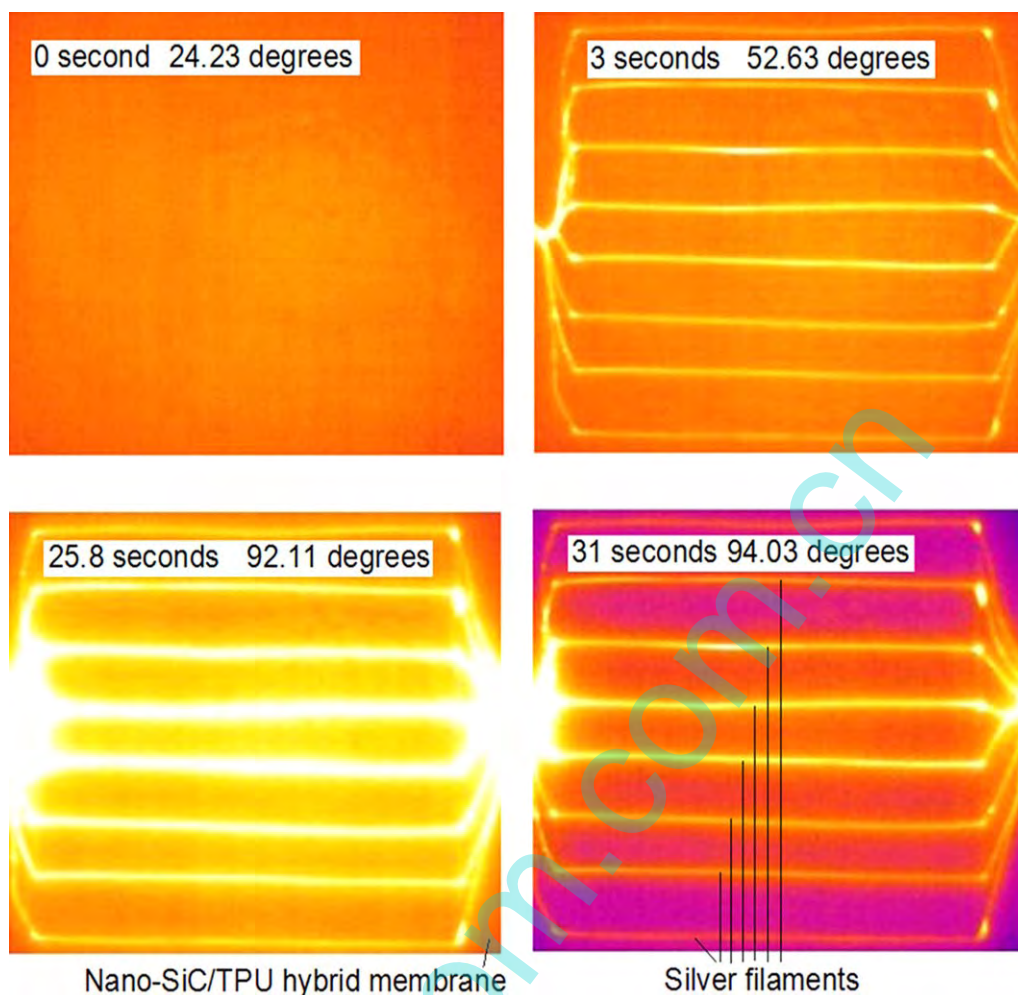


**Figure 10.** Infrared temperature images of nano-SiC(10 wt %)/TPU membrane at 4 V loaded voltage. [Color figure can be viewed in the online issue, which is available at [wileyonlinelibrary.com](http://wileyonlinelibrary.com).]

macromolecular structure, therefore, the stress of nano-SiC/TPU hybrid membrane will decrease. The breaking elongation at break of nano-SiC/TPU hybrid membrane decreases with increasing of nano-SiC as a whole, Initial modulus of nano-SiC/TPU hybrid membrane is hardly correlation with nano-SiC content.

Figure 8 shows surface maximum temperature of nano-SiC (10 wt %)/TPU hybrid membrane increases with loaded voltage:

$$\phi = \lambda A \frac{\Delta t}{\delta} + h \Delta t + \varepsilon \sigma T^4 \quad (1)$$

where  $\phi$  denotes total thermal flow,  $\lambda$  denotes heat conductivity coefficient,  $A$  denotes heat conductivity area,  $\delta$  denotes thickness of material,  $h$  denotes heat convection coefficient,  $\varepsilon$  denotes emissivity,  $\sigma$  denotes Stefan-Boltzmann constant, and  $T$  denotes thermodynamic temperature of material.

Three kinds of heat transfer approaches, such as heat conduction, heat convection and heat radiation, are exhibited in right of eq. (1), amount of heat transfer  $Q$  is exhibited in left of eq. (1). The heat is produced in silver filament is a constant because of constant loaded voltage and constant resistance.

Temperature difference between silver filament and environment is small,  $\phi$  is far less than  $Q$ , hence surface temperature on silver filament ascend sharply at the beginning of heating. Surface temperature on silver filament reaches maximum value when  $\phi$  is equal to  $Q$ . Equation (1) provides theory for simulating temperature change process of silver filament or heating membranes.

Figure 9 shows the overall view of flexible heating membrane with 10 wt % nano-SiC particles. The area of membrane is  $43.2 \text{ cm}^2$ , and the distance between silver filaments is 8 mm, surface of heating membrane is smooth, silver filaments are enclosed in nano-SiC/TPU hybrid membrane which can prevent short circuit because of sweat. Figure 10 shows the infrared temperature images at different moment when loaded voltage is 4 V, the surface temperature ascends with time and finally reaches maximum temperature. The maximum temperature of heating membrane went up  $28.4^\circ\text{C}$  in initial 3 seconds, after heating 25.8 seconds, the maximum temperature of heating membrane only went up  $1.92^\circ\text{C}$  in 5.2 seconds. Moreover, we can observe that the surface temperature of silver filaments at the edge of membranes is lower than that of silver filaments at



the center of membranes, the reason is that silver filaments at the edge of membranes have more length and bigger resistance than silver filaments at center of membrane, the current flowing silver filaments at the edge of heating membranes is smaller than that of silver filaments at the center of heating membranes. Too large temperature difference between silver filaments will affect the heating effect of heating membrane which should be prevented by well layout design.

## CONCLUSIONS

This article presented a method for fabricating flexible, waterproof nano-SiC/TPU heating membranes, organo-functional groups were successfully grafted on nano-SiC particles by surface modification. Modified nano-SiC particles can be dispersed evenly into DMF solvent. TPU membrane with 10 wt % nano-SiC has the best thermal stability and mechanical properties. The thermal conduction coefficient of TPU hybrid membranes increase with increasing of nano-SiC, and the infrared temperature images shows surface temperature of nano-SiC/TPU hybrid membranes ascends rapidly at the beginning of loading voltage, then reaches gradually equilibrium temperature. Giving the same loaded voltage, the heat energy on silver filament can transfer faster to surface of hybrid membrane with increasing of nano-SiC. Flexible, waterproof nano-SiC/TPU heating membranes have wide application prospect in active warming garments and other fields required flexible heating elements.

## ACKNOWLEDGMENTS

The authors would like to thank the National Natural Science Foundation of China (Grant No. 51473122, 51102178, 51173131), Tianjin City High School Science & Technology Fund Planning Project (Grant No. 20120321, 20130324), and Tianjin Research Program of Application Foundation and Advanced Technology (Key Project of Natural Science Foundation) (No.13JCZDJC32500) for support of the work reported in this article.

## REFERENCES

1. Bonato, P. *IEEE Eng. Med. Biol. Mag.* **2010**, 29, 25.
2. Lymberis, A.; Dittmar, A. *IEEE Eng. Med. Biol. Mag.* **2007**, 26, 29.
3. Liu, H.; Tao, X. M.; Xu, P. J.; Zhang, H.; Bai, Z. Q. *Measurement* **2013**, 46, 1904.
4. Hewitt, F. W. Electric heating pad and fabric, 1929, patent number 1703005.
5. André, B. de la Bretonière. Electric heating fabric, 1985, Patent Number 4,538,054.
6. Cristian, I.; Nauman, S.; Cochrane, C.; Koncar, V. *Advances in Modern Woven Fabric Technology*, **2011**, 1.
7. Liu, H.; Zhang, Y.; Chen, L.; Li, X. J.; Wang, Y. X.; Gao, Y. *Measurement* **2012**, 45, 1865.
8. Hamdani, S. T. A.; Potluri, P.; Fernando, A. *Materials* **2013**, 6, 1072.
9. Bian, J.; Lin, H. L.; He, F. X.; Wei, X. W.; Chang, I. T.; Sancaktar, E. *Compos. A Appl. Sci. Manuf.* **2013**, 47, 72.
10. Ganguli, S.; Roy, A. K.; Anderson, D. P. *Carbon* **2008**, 46, 806.
11. Veca, L. M.; Meziani, M. J.; Wang, W.; Wang, X.; Lu, F.; Zhang, P.; Sun, Y. P. *Adv. Mater.* **2009**, 21, 2088.
12. Han, Z.; Fina, A. *Prog. Polym. Sci.* **2011**, 36, 914.
13. Kumlutaş, D.; Tavman, I. H.; Turhan Çoban, M. *Compos. Sci. Technol.* **2003**, 63, 113.
14. Boudenne, A.; Ibos, L.; Fois, M.; Majesté, J. C.; Géhin, E. *Compos. A Appl. Sci. Manuf.* **2005**, 36, 1545.
15. Cao, J. P.; Zhao, J.; Zhao, X.; Hu, G. H.; Dang, Z. M. *J. Appl. Polym. Sci.* **2013**, 130, 638.
16. Saha, C.; Chaki, T. K.; Singha, N. K. *J. Appl. Polym. Sci.* **2013**, 130, 3328.
17. Iqbal, M.; McCullough, M.; Harris, A.; Eichhorn, S. H. *J. Therm. Anal. Calorim.* **2012**, 108, 933.
18. Zhou, T.; Wang, X.; Mingyuan, G. U.; Liu, X. *Polymer* **2008**, 49, 4666.
19. Choi, S.; Im, H.; Kim, J. *Compos. A Appl. Sci. Manuf.* **2012**, 43, 1860.
20. Raman, C.; Meneghetti, P. *Plastics, Additives Compounding* **2008**, 10, 26.
21. Ohashi, M.; Kawakami, S.; Yokogawa, Y.; Lai, G. C. *J. Am. Ceram. Soc.* **2005**, 88, 2615.
22. Mu, Q.; Feng, S.; Diao, G. *Polym. Compos.* **2007**, 28, 125.
23. Gu, J.; Zhang, Q.; Dang, J.; Zhang, J.; Yang, Z. *Polym. Eng. Sci.* **2009**, 49, 1030.
24. Zhou, W.; Qi, S.; An, Q.; Zhao, H.; Liu, N. *Mater. Res. Bull.* **2007**, 42, 1863.